Conventional and advanced brain MR imaging in patients with sickle cell anemia

Pratibha Issar, Maya Nehra, Gurmeet Singh[1], SK Issar[2]

Departments of Radiodiagnosis, [1]Hematology and [2]Gastroenterology, J.L.N. Hospital and Research Centre, Bhilai, Chhattisgarh, India

Correspondence: Dr. Pratibha Issar, Department of Radiodiagnosis, J.L.N. Hospital and R.C, Bhilai - 490 009, Chhattisgarh, India.
E-mail: mareesh_23@yahoo.co.in

Abstract

Background: Sickle cell disease (SCD) is an autosomal recessive hemolytic disorder; its cerebrovascular complications include silent cerebral ischemia, infarct, and brain atrophy. Conventional magnetic resonance imaging (MRI) often underestimates the extent of injury. Diffusion tensor imaging (DTI) can demonstrate and quantify microstructural brain changes in SCD cases having normal routine MRI. **Objective:** To identify various neurological abnormalities in asymptomatic sickle cell patients using routine MRI and to evaluate the microstructure of various regions of the brain using DTI. **Materials and Methods:** A prospective, randomized case–control study was conducted over a period of 2 years. A total of 58 cases of SCD and 56 age- and sex-matched controls were included. Routine MRI and DTI were performed in both the groups following a standard protocol. Fractional anisotropy (FA) and apparent diffusion coefficient (ADC) were calculated in certain pre-defined regions. Primary data were analyzed using MS excel version 17. Analysis of variance test was performed and statistical significance was set at $P < 0.05$. **Results:** Thirty regions of interest with 60 variables were included in the final analysis. Patients with SCD showed statistically significant reduced FA values, increased ADC values, or both, clustered in several brain areas, including pons, cerebral peduncle, corpus callosum, frontal, temporal, parietal white matter, centrum semiovale, periventricular areas, basal ganglia, and left thalamus ($P < 0.05$). **Conclusion:** DTI is a promising method for characterizing microstructural changes, when conventional MRI is normal.

Key words: Apparent diffusion coefficient; diffusion tensor imaging; fractional anisotropy; sickle cell disease; sickle cell anemia; sickle cell trait

Introduction

Sickle cell disease (SCD) is a hereditary red blood cells' disorder characterized by a point mutation in the sixth position of the β-chain of the hemoglobin molecule in which valine is substituted for glutamic acid leading to the formation of defective hemoglobin in the erythrocytes. When deprived of oxygen, sickle cell molecules undergo polymerization, a process sometimes called gelation or crystallization. The change in the physical state of sickle hemoglobin distorts red blood cell and turns it into a sickle shape. These sickled and rigid cells lack the flexibility required to flow in the circulation, leading to vasoocclusion, ischemia, and infarcts. Normal hemoglobin has two α- and two β-globin chains. If both the β-globin chains are defective, the disease is called homozygous hemoglobin sickle cell anemia (SCA) (HbSS),

whereas the heterozygous variant is known as sickle cell trait (SCT) (HbAS).[1-3]

SCD can affect many organs in the body, but brain injury is one of the most devastating and feared complications leading to mortality and morbidity. The cerebrovascular complications of SCD include stroke, transient ischemic attack, silent cerebral ischemia (SCI), and brain atrophy. SCI is defined by areas of increased signal intensity on FLAIR T2-weighted images of the brain in the absence of overt clinical neurologic symptoms. SCI typically occurs at the watershed border zones of vascular territories, which are supplied by smaller endarterial branches and therefore vulnerable to ischemia. Sickle cell vasculopathy can involve both large and small vessels, although typically the terminal internal carotid artery (ICA), proximal anterior cerebral artery (ACA), and middle cerebral artery (MCA) are affected leading to stenosis. Over time and with progressive occlusion of the main intracranial arteries, a so-called "Moya Moya" (Japanese: puff of smoke) appearance is seen, which is characterized by the formation of numerous tiny collaterals. MR angiography (MRA) can easily detect vascular narrowing, occlusion, and collateral formation. Intracranial hemorrhage is a rare but significant complication of the disease which can be demonstrated by susceptibility weighted imaging(SWI).[4-6]

Conventional magnetic resonance imaging (MRI) cannot precisely delineate microstructural changes in the white matter fiber tracts of the brain. Diffusion tensor imaging (DTI) is an emerging MRI-based technique that is often used in research to study the white matter fiber tracts. The principle of DTI is to analyze the multiple diffusion-sensitizing gradient directions which measure the Brownian motion of water molecules in biologic tissue which can detect and quantify microstructural brain changes earlier than conventional MRI. This novel technique is able to show the orientation and integrity of white matter fibers *in vivo*. The apparent diffusion coefficient (ADC) is a measure of the degree of restriction to water diffusion, and fractional anisotropy (FA) is a measure of preponderant directionality of water diffusion. These two parameters are the most frequently used DTI metrics for measuring microstructural tissue damage in patients with brain disease. Recent studies using DTI have shown detection of abnormalities in cerebral parenchyma in SCD. It is therefore a non-invasive neuroimaging technique to detect the cerebrovascular injuries in SCD. This study intends to evaluate the cerebral morphology of asymptomatic patient diagnosed with SCD using conventional and diffusion tensor MRI to statistically validate the above notion.[7-9] However, the fact that SCD cases who have normal MRI findings can still be cognitively impaired suggests that there is a diffuse brain injury in these patients. The aim of this study was to evaluate the microstructure of various regions of the brain using DTI in asymptomatic patients of SCD with age- and sex-matched controls.

Materials and Methods

This study was a "prospective observational case–control study" conducted over 2 years, from January 2015 to December 2016. The study included 58 SCD (SCA 40, SCT 18) cases having no neurological problem and 56 healthy controls. The control group included subjects of the same age (±2 years). Demographic profile of cases and controls is given in Table 1.

Ethical clearance was taken from the Institutional Ethical Committee. Inclusion criteria for the cases were neurologically asymptomatic cases of SCA or SCT. The control group included healthy subjects in the age group 11–55 years. Exclusion criteria were patients with SCD with abnormal neurological examination or a history of stroke. Informed consent was taken from both the case and control groups before the procedure. There is no conflict of interest.

Data Acquisition

All brain MR imaging data were acquired from a 1.5-T MR Imaging scanner (Signa Excite; GE Healthcare, Milwaukee, WI, USA) using an eight-channel phased-array head coil and a gradient system with a slew rate of 120 mT/m/s and a maximum gradient amplitude of 33 mT/m. None of the study participants required sedation or general anesthesia to undergo the procedure. After triplaner scans and acquisition of calibration data, axial T1 WI, T2 WI, T2-FLAIR, sagittal T1-FLAIR, DWI, three-dimensional (3D) TOF MRA, and SWI sequences were acquired from each subject. Images from these sequences were used to diagnose pre-existing lesion in patients, and those who had lesion diagnosed were excluded from comparative DTI study.

DTI data were acquired using echo planer imaging with a data acquisition matrix of 128 × 128, field of view (FOV) of 26 × 24, TR/TE of 10000/99, flip angle 90°, and NEX of 2. Contiguous 3-mm-thick slices with no interslice gap were acquired in the axial direction covering the whole brain. The protocol comprises 25 diffusion gradient directions with b value of 0 and 1000 s/mm^2 The mean acquisition time for DTI was approximately 10 min 30 s and 20 min for DTI data processing.

Table 1: Demographic profile

Sex	SCA	SCT	Control
Male	18 (14-32 years)	11 (13-48 years)	32 (13-50 years)
Female	22 (13-38 years)	7 (15-54 years)	24 (11-55 years)
Total	40	18	56

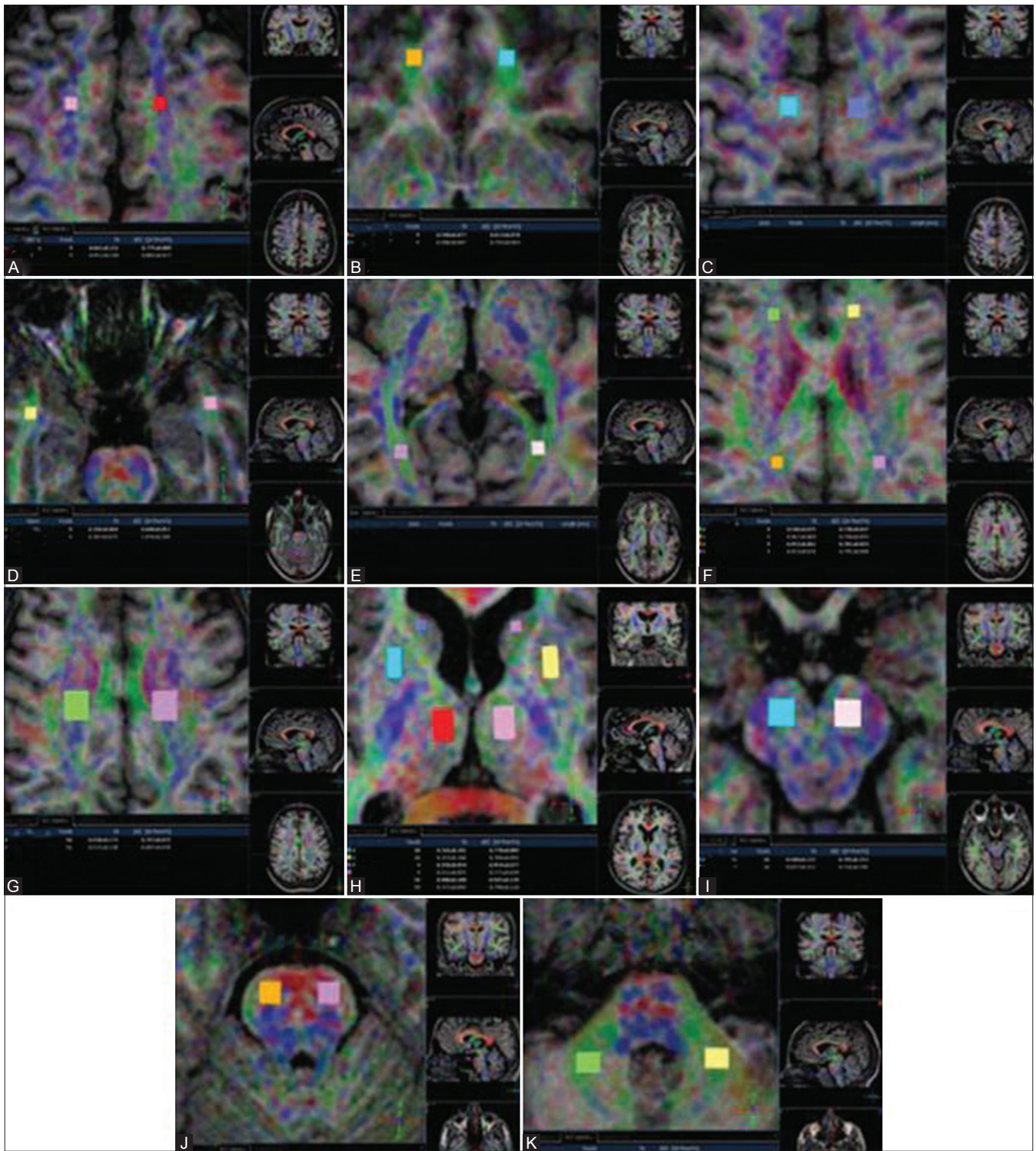SCA: sickle cell anemia, SCT: sickle cell trait

Figure 1 (A-K): Region-of-interest analysis of fractional anisotropy (FA) and apparent diffusion coefficient values for various brain tissues on FA maps images. A–K, Superior frontal white matter (A), inferior frontal white matter (B), parietal white matter (C), temporal white matter (D), occipital white matter (E), periventricular white matter areas (F), centrum semiovale (G), basal ganglia and thalamus (H), cerebral peduncle (I), pons (J), and cerebellar white matter (K)

DTI data were transferred to a commercially available work station Adw 4.4. All images were first visually inspected for apparent artefacts, auto correction was done, and DTI-based color map was generated.

Quantitative analysis was performed by outlining regions of interest (ROIs) on FA maps with size ranging from 4 pixels (2 × 2) and 40 pixels (8 × 5). Standard square to rectangle symmetric ROIs were used for

analysis of FA and ADC according to anatomic shape of the brain area.

The routine images were analyzed and reported initially by a junior radiologist with 3 years of experience, which was followed by a repeat examination and validation by a senior radiologist with 10 years of experience. Quantitative analysis of FA and ADC maps was done by manually drawing ROI on axial images on various brain areas: superior and inferior frontal, parietal, occipital, and temporal white matter areas, anterior and posterior periventricular areas, centrum semiovale, basal ganglia (lentiform nucleus, head of caudate nucleus), thalamus, cerebral peduncles, pons, cerebellar white matter, and corpus callosum (CC) [Figure 1].

Superior and inferior frontal white matter ROIs were drawn on the axial slice that was at the level of five slices superior to the superior edge of CC and at the level of inferior edge of rostrum, respectively. Parietal white matter ROIs were also placed at the same slice of superior frontal white matter. The ROIs of occipital white matter, basal ganglia, and thalamus were drawn at the level of inferior edge of splenium. The ROIs of temporal white matter were at the level of inferior edge of frontal lobe. The ROIs of posterior and anterior periventricular areas were drawn at the level of the roof of lateral ventricle. For CC at the level of frontal horn and atrium of lateral ventricle, mid line in genu, and splenium region. The ROIs of the cerebral peduncle and pons were at the level of optic chiasm and superior cerebellar peduncle, respectively. Cerebellar white matter ROIs were drawn at the level of inferior edge of pons.[7,8]

After primary data collection, a master chart was prepared with the help of Microsoft Excel sheet and analyzed using MS Excel (Statistical Package for Social Sciences) version 17. Analysis of variance test was performed for determination of statistically significant differences in particular variables between the patient and control groups. Statistical significance was set at $P < 0.05$.

Results

Conventional MRI findings

The conventional MRI of the control subjects was normal. Two patients with SCA showed T2 and T2-FLAIR hyperintensity in deep white matter, which did not show restriction on DWI. The first patient was a 38-year-old female having T2-FLAIR linear hyperintensity in deep white matter of left frontal lobe [Figure 2]. Another patient was an 18-year-old female with SCA having small T2-FLAIR hyperintensity in deep white matter of right frontal lobe.

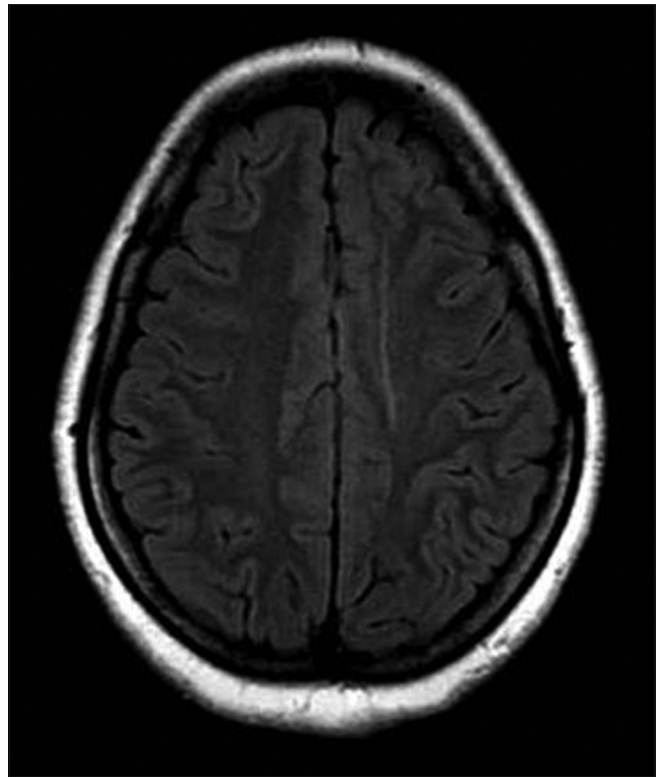MRA did not reveal any stenosis or occlusion. SWI images were unremarkable.

Figure 2: Axial T2 Flair image in 38 year-old female SCD patient, showing linear hyperintensity in deep white matter of left frontal region suggestive of silent cerebral ischemia

Diffusion tensor imaging region-of-interest analysis

All DTI images were inspected visually for echo-planer imaging-related susceptibility artifacts and geometric distortion, after EPI distortion correction, color, and grey map were generated. In all 30 ROIs with 60 variables, that is, FA and ADC values for each region, were analyzed and compared with the corresponding contra-lateral area of same patient and with comparable area of controls. The average of all ROIs of different regions in SCD, SCT, and control were taken out. The FA values showed a statistically significant difference between patients with SCD and control subjects in CC genu (0.605 vs 0.668, $P = 0.003$), splenium (0.596 vs 0.650, $P = 0.005$), left centrum semiovale (0.413 vs 0.471, $P = 0.001$), anterior periventricular white matter left side (0.380 vs 0.456, $P = 0.007$), posterior periventricular white matter left side (0.366 vs 0.477, $P = 0.004$), pons left (0.414 vs 0.495, $P = 0.001$), head of caudate nucleus left (0.293 vs 0.615, $P = 0.001$), and lentiform nucleus left (0.304 vs 0.502, $P = 0.001$). The remaining areas with decreased FA values are given in Table 2.

ADC values showed a statistically significant difference between patients with SCD and control subjects in the CC genu (0.917 vs 0.831, $P = 0.001$), right caudate nucleus (0.842 vs 0.771, $P = 0.001$), left caudate nucleus (0.853 vs 0.778, $P = 0.001$), left thalamus (0.837 vs 0.794, $P = 0.001$), and right and left pons (0.863 vs 0.825, $P = 0.013$ and 0.867

Table 2: FA value comparison in SCD, SCT, and control

Region of measurements	SCD	SCT	Control	P	Remarks
Pons (right)	0.4317±0.0541	0.4364±0.0289	0.4854±0.04072	0.001	Significant
Pons (left)	0.4143±0.0356	0.4207±0.05563	0.4950±0.0884	0.001	Significant
Cerebellar white matter (right)	0.4707±0.08827	0.4888±0.13221	0.4671±0.02781	0.480	
Cerebellar white matter (left)	0.4643±0.08786	0.4733±0.12304	0.4653±0.04105	0.887	
Cerebral peduncle (right)	0.4810±0.0865	0.5043±0.0694	0.5252±0.0550	0.011	Significant
Cerebral peduncle (left)	0.4810±0.1131	0.4893±0.0720	0.5389±0.0585	0.003	Significant
Inf. frontal white matter (right)	0.3217±0.04384	0.3507±0.04287	0.4409±0.03559	0.001	Significant
Inf. frontal white matter (left)	0.3331±0.06303	0.3564±0.08326	0.4448±0.0400	0.002	Significant
Temporal white matter (right)	0.3886±0.09020	0.3990±0.08263	0.4796±0.04805	0.002	Significant
Temporal white matter (left)	0.4300±0.07599	0.4386±0.06781	0.4870±0.05325	0.001	Significant
Head of caudate nucleus (right)	0.2895±0.09748	0.3150±0.13455	0.6170±0.0827	0.002	Significant
Head of caudate nucleus (left)	0.2933±0.08461	0.3171±0.12288	0.6150±0.0959	0.001	Significant
Lentiform nucleus (right)	0.3014±0.0933	0.3007±0.11371	0.4993±0.0441	0.004	Significant
Lentiform nucleus (left)	0.3048±0.09969	0.3086±0.1237	0.5021±0.0376	0.001	Significant
Thalamus (right)	0.5281±1.2478	0.3798±0.10183	0.4737±0.07591	0.796	
Thalamus (left)	0.3433±0.064790	0.3829±0.09393	0.4798±0.06527	0.001	Significant
Occipital white matter (right)	0.5805±1.24660	0.4229±0.05165	0.4586±0.06357	0.669	
Occipital white matter (left)	0.3929±0.08306	0.4100±0.4472	0.4711±0.05399	0.001	Significant
Superior frontal white matter (right)	0.3664±0.0960	0.3771±0.0571	0.4914±0.0530	0.001	Significant
Superior frontal white matter (left)	0.3476±0.0707	0.3750±0.0443	0.4866±0.0341	0.001	Significant
Parietal white matter (right)	0.4013±0.0743	0.4336±0.0789	0.4772±0.0344	0.001	Significant
Parietal white matter (left)	0.40114±0.0653	0.4192±0.0583	0.4766±0.04162	0.001	Significant
Anterior periventricular (right)	0.3714±0.04842	0.3979±0.04191	0.4472±1.52504	0.002	Significant
Anterior periventricular (left)	0.3805±0.04747	0.4329±0.04598	0.4562±0.03897	0.007	Significant
Posterior periventricular (right)	0.3660±0.04696	0.3807±0.04615	0.4811±0.05704	0.001	Significant
Posterior periventricular (left)	0.3664±0.04433	0.3821±0.04577	0.4779±0.04631	0.004	Significant
Centrum semiovale (right)	0.4214±0.07131	0.4121±0.06253	0.4612±0.03977	0.003	Significant
Centrum semiovale (left)	0.4136±0.05286	0.4369±0.06820	0.4711±0.03273	0.001	Significant
Corpus callosum genu	0.6057±0.02821	0.6114±0.03280	0.6686±0.04630	0.003	Significant
Corpus callosum splenium	0.5964±0.03992	0.6326±0.04019	0.650±0.04158	0.005	Significant

SCA: sickle cell anemia, SCT: sickle cell trait

vs 0.827 $P = 0.017$). The remaining areas with increased ADC values are mentioned in Table 3.

Two patients with SCA with silent infarct, when compared to without infarct ones, have lower FA in right (0.312 vs 0.366) and left (0.321 vs 0.347) along with high ADC value in right (0.832 vs 0.774) and left (0.829 vs 0.802) superior frontal region.

Discussion

Brain injury in SCD is diffuse and insidious, and conventional neuroimaging often underestimates the extent of injury. In this study, we compared FA and ADC values in different areas of brain in SCA (homozygous) and SCT (heterozygous) with normal control subjects. We had 40 cases of SCA, 18 of SCT, and 56 normal age- and sex-matched control. Two cases of SCA having SCI were excluded from DTI study. In these two cases, DTI values were taken separately. Due to age-related alterations in white matter micro structure in DTI studies, we have

included controls in the same age range as that of cases in this study.

Conventional MRI findings

Two cases of SCA (4%) showed T2-FLAIR hyperintensity, suggestive of SCI. Both patients had T2-FLAIR hyperintensity in deep white matter. The deep white matter is perfused by arterioles and is more liable to inadequate perfusion and subsequent infarction. Small-vessel disease in SCD is due to the formation of intravascular masses of dense or less flexible sickled erythrocytes in peripheral arterioles and post capillary venules. FLAIR sequence is one of the most reliable conventional MRI acquisition techniques for assessing the presence of SCI.[10-12]

Previous studies have defined stenosis as obvious narrowing or focal signal dropout in a major artery and occlusion as signal loss from the distal portion of a major artery.[2,5] In our study on MRA, no evidence of any stenosis or occlusion was observed.

Table 3: Comparison of ADC values in SCD, SCT, and control

Region of measurements	SCD	SCT	Control	P	Remarks
Pons (right)	0.863±0.065	0.840±0.060	0.825±0.063	0.013	Significant
Pons (left)	0.827±0.065	0.840±0.066	0.867±0.066	0.017	Significant
Cerebellar white matter (right)	0.827±0.064	0.801±0.0708	0.780±0.052	0.001	Significant
Cerebellar white matter (left)	0.838±0.0572	0.810±0.061	0.777±0.0455	0.001	Significant
Cerebral peduncle (right)	0.881±0.058	0.870±0.047	0.843±0.060	0.006	Significant
Cerebral peduncle (left)	0.871±0.055	0.871±0.0424	0.841±0.046	0.004	Significant
Inf. frontal white matter (right)	0.855±0.473	0.780±0.2145	0.832±0.0856	0.015	Significant
Inf. frontal white matter (left)	0.855±0.7302	0.859±0.061	0.833±0.0442	0.121	
Temporal white matter (right)	0.878±0.692	0.885±0.064	0.774±0.046	0.001	Significant
Temporal white matter (left)	0.864±0.063	0.743±0.7666	0.773±0.0515	0.001	Significant
Head of caudate nucleus (right)	0.842±0.034	0.830±0.0667	0.771±0.060	0.001	Significant
Head of caudate nucleus (left)	0.853±0.0347	0.854±0.0497	0.778±0.063	0.001	Significant
Lentiform nucleus (right)	0.809±0.126	0.822±0.03296	0.829±0.0264	0.478	
Lentiform nucleus (left)	0.826±0.03902	0.828±0.03254	0.826±0.030	0.972	
Thalamus (right)	0.823±0.13276	0.842±0.0333	0.874±0.490	0.779	
Thalamus (left)	0.837±0.0414	0.824±0.045	0.794±0.0559	0.001	Significant
Occipital white matter (right)	0.823±0.133	0.839±0.030	0.814±0.087	0.271	
Occipital white matter (left)	0.831±0.134	0.854±0.0241	0.822±0.088	0.145	
Superior frontal white matter (right)	0.832±0.047	0.834±0.048	0.813±0.042	0.027	Significant
Superior frontal white matter (left)	0.829±0.038	0.821±0.046	0.816±0.057	0.475	
Parietal white matter (right)	0.867±0.057	0.859±0.045	0.834±0.04	0.003	Significant
Parietal white matter (left)	0.859±0.050	0.846±0.039	0.832±0.040	0.018	Significant
Anterior periventricular (right)	0.824±0.051	0.803±0.040	0.761±0.204	0.149	
Anterior periventricular (left)	0.793±0.012	0.801±0.044	0.811±0.038	0.562	
Posterior periventricular (right)	0.851±0.058	0.841±0.048	0.832±0.047	0.113	
Posterior periventricular (left)	0.870±0.050	0.835±0.049	0.831±0.052	0.043	Significant
Centrum semiovale (right)	0.820±0.0263	0.801±0.021	0.827±0.0356	0.023	Significant
Centrum semiovale (left)	0.821±0.0341	0.828±0.033	0.749±0.213	0.005	Significant
Corpus callosum genu	0.917±0.056	0.890±0.063	0.831±0.034	0.001	Significant
Corpus callosum splenium	0.880±0.052	0.879±0.050	0.840±0.039	0.001	Significant

SCA: sickle cell anemia, SCT: sickle cell trait

Intracranial hemorrhage is a know complication of SCD. Bleeding may be parenchymal, subarachnoid, or intraventricular. None of our patients had intracranial and micro-hemorrhages in SWI images. This may be possible as all our cases were asymptomatic.[6,13]

Diffusion tensor imaging findings

In this study, a wide range of bilateral changes in FA and ADC values were observed in patients with SCD compared with healthy control subjects. Using an ROI-based analytic approach, the results of this study indicate significantly reduced FA values, increased ADC values, or both for patients with SCD clustered in different areas of brain, CC, frontal white matter, centrum semiovale, periventricular areas, and head of the caudate nucleus, thalamus, cerebral peduncle, and pons. Bilaterally decreased FA and increased ADC values were the findings in patients with SCD compared with healthy control subjects in almost all brain areas measured even if the difference was without statistical significance.

The difference in FA and ADC values was observed in SCD between the right and the left sides of the brain in certain areas such as temporo-occipital white matter, periventricular, central semiovale, and thalamic region. These asymmetries can be explained by the fact that there are microstructural changes secondary to vascular involvement in different severities between the two hemispheres. Two patients of SCD with silent ischemia had significantly lower FA values and higher ADC values in various brain areas. This finding suggests that this subgroup of patients with SCD has more severe microstructural changes than patients with SCD without silent infarct.[14-16]

Reduction in FA and an increase in ADC values were noticed in patients with SCD as compared with SCT as the severity of disease is more in homozygous cases. Myelination, axonal water, and packing of axonal fibers all affect the ADC in the brain tissue. The loss of myelinated axons may cause loosing of anatomic barriers to water diffusion and may result in increased ADC

values. Reduced FA can be caused by reduced axons per cross-sectional area, reduced axonal calibre and density, or decreased myelin.[17] In our study, the FA changes are attributable to axonal damage in the brain tissue that is exposed to chronic ischemia. The increase in ADC values may represent increased extracellular water content secondary to gliosis and to micro and macroscopic cystic changes in the brain. These findings are consistent with the results reported in chronic ischemia. Decreased FA, increased ADC, or both were not only in CC, basal ganglia, or lobar white matter areas but also in cerebral peduncle and pons, suggesting patients with SCD have global brain involvement. We excluded from ROI analysis the ischemic changes that were visible on conventional MR sequences. This proves that various brain areas without visible signal intensity changes on conventional MRI are also vulnerable to ischemic damage.

Conclusion

We conclude that decrease in FA and increase in ADC found in various brain regions without visible signal intensity changes on conventional MRI in patients with SCD are associated with microstructural changes consistent with axonal damage due to vasculopathy. DTI can be used as a sensitive marker to quantify brain tissue alterations in patients with SCD. Longitudinal studies with DTI may help in monitoring the neurological involvement in SCD.

Financial support and sponsorship
Nil.

Conflicts of interest
There are no conflicts of interest.

References

1. Darghouth D, Koehl B, Madalinski G, Heilier J-F, Bovee P, Xu Y, *et al*. Pathophysiology of sickle cell disease is mirrored by the red blood cell metabolism. Blood J 2011;117:1-4.

2. Abboud MR, Cure J, Granger S, Gallagher D, Hsu L, Wang W, *et al*. Magnetic resonance angiography in children with sickle cell disease and abnormal transcranial Doppler ultrasonography findings enrolled in the STOP study. Blood 2014;103:2822-6.

3. Panigrahi S, Patra PK, Khodiar PK. The screening and morbidity pattern of sickle cell anemia in Chhattisgarh. Indian J Hematol Blood Transfus 2015;31:104-9.

4. Moser FG, Miller ST, Bello JA, Pegelow CH, Zimmerman RA, Wang WC, *et al*. The spectrum of brain MR abnormalities in sickle-cell disease: A report from the Cooperative Study of Sickle Cell Disease. Am J Neuroradiol1996;17:965-72.

5. Kotb MM, Tantawi WH, Elsayed AA, Damanhouri GA, Malibary HM. Brain MRI and CT findings in sickle cell disease patients from Western Saudi Arabia Neuroscience. 2006;11:28-36.

6. Haacke EM, Mittal S, Wu Z, Neelavalli J, Cheng YCN. Susceptibility-weighted imaging: Technical aspects and clinical applications, part 1. Am J Neuroradiol 2009;30:19-30.

7. Balci A, Karazincir S, Beyoglu Y, Cingiz C, Davran R, Gali E, *et al*. Quantitative brain diffusion-tensor MRI findings in patients with sickle cell disease. Am J Roentgenol 2012;198:1167-74.

8. Sun B, Brown RC, Hayes L, Burns TG, Huamani J, Bearden DJ, *et al*. White matter damage in asymptomatic patients with sickle cell anemia: Screening with diffusion tensor imaging. Am J Neuroradiol 2012;33:20439.

9. Wakana S, Jiang H, Nagae-Poetscher LM, van Zijl PCM, Mori S. Fiber tract-based atlas of human white matter anatomy. Radiology 2004;230:77-87.

10. Thust SC, Burke C, Siddiqui A. Neuroimaging findings in sickle cell disease. Br J Radiol 2014;87:20130699 (1-8)

11. Kawadler JM, Kirkham FJ, Clayden JD, Hollocks MJ, Seymour EL, Edey R, *et al*. White matter damage relates to oxygen saturation in children with sickle cell anemia without silent cerebral infarcts. Stroke 2015;46:1793-9.

12. Steen RG, Emudianughe T, Hankins GM, Wynn LW, Wang WC, Xiong X, *et al*. Brain imaging findings in pediatric patients with sickle cell disease. Radiology 2003;228:216-25.

13. Winchell AM, Taylor BA, Song R, Loeffler RB, Grundlehner P, Hankins JS, *et al*. Evaluation of SWI in children with sickle cell disease. Am J Neuroradiol 2014;35:1016-21.

14. Jellison BJ, Field AS, Medow J, Lazar M, Salamat MS, Alexander AL. Diffusion tensor imaging of cerebral white matter: A pictorial review of physics, fiber tract anatomy and tumor imaging patterns. Am J Neuroradiol 2004;25:356-69.

15. Pagelow CH, Macklin EA, Moser FG, Wang WC, Bello JA, Miller ST, *et al*. Longitudinal changes in brain magnetic resonance imaging findings in children with sickle cell disease. Blood 2002;99:3014-8.

16. Chen R, Arkuszewski M, Krejza J, Zimmerman RA, Herskovits EH, Melhem ER. A prospective longitudinal brain morphometry study of children with sickle cell disease. Am J Neuroradiol 2015;36:403-10.

17. Beaulieu C. The basis of anisotropic water diffusion in the nervous system: a technical review. NMR Biomed 2002;15:43555.